arXiv:math-ph/0406025v2 24 Jul 2004

Raise and Peel Models of fluctuating interfaces and combinatorics of Pascal's hexagon

P. Pyatov[1]

Bogoliubov Laboratory of Theoretical Physics, JINR
141980 Dubna, Moscow Region, Russia

Abstract.

The raise and peel model of a one-dimensional fluctuating interface (model A) is extended by considering one source (model B) or two sources (model C) at the boundaries. The Hamiltonians describing the three processes have, in the thermodynamic limit, spectra given by conformal field theory. The probability of the different configurations in the stationary states of the three models are not only related but have interesting combinatorial properties. We show that by extending Pascal's triangle (which gives solutions to linear relations in terms of integer numbers), to an hexagon, one obtains integer solutions of bilinear relations. These solutions give not only the weights of the various configurations in the three models but also give an insight to the connections between the probability distributions in the stationary states of the three models. Interestingly enough, Pascal's hexagon also gives solutions to a Hirota's difference equation.

1 Introduction.

Recently much interest have been devoted to surprising appearence of the ASM (alternating sign matrices) combinatorics in the properties of the ground state wave function of XXZ spin chain at a particular value $\Delta = -1/2$ of its anisotropy [1]. In subsequent investigations [2]–[12] a number of models having ground states with interesting combinatorial properties was found, including the dense O(1) loop model, the rotor model and the "raise and peel" model of fluctuating interface. Two important facts are common for these models. First, all they admit a purely algebraic description in terms of an appropriate version of a (quotient of) Temperley–Lieb (TL) algebra (see [10]). Secondly, the TL algebras always come in a very specific semigroup regime. This latter fact was used in [5, 10] to interpret the loop model as a stochastic process and thus, to give a physical interpretation to the components of the ground state wave function as (unnormalized) probabilities of various configurations.

In the present paper we extend the raise and peel model[2] (hereafter called model A) obtained for the TL algebra to two other cases. In order to do so, we consider the boundary

[1]E-mail: pyatov@thsun1.jinr.ru

[2]For detailed discussion of physical properties of the raise and peel model the reader is referred to papers [12, 13].

extension of the TL algebra which is called the blob algebra [14, 15, 11] (see Section 2). In this way, in the stochastic model one can introduce a source at one boundary (model B) or sources at the two boundaries (model C). The two new models are described in detail in Section 3. As shown in Ref.[16], in the continuum limit, the spectra of the two Hamiltonians giving the time evolution of the stochastic processes are given by characters of N=2 superconformal field theory. Here we are going to consider the combinatorial properties of the stationary states only.

In Section 4, based on numerical studies of small chains we make a series of conjectures for the weights of various configurations observed in the stationary states of the three models. In Appendix A we define Pascal's hexagon. We think that the content of this Appendix is interesting on its own. Using Pascal's hexagon one can get in a simple way the numerical results obtained for the stationary states for finite systems (see Section 4).

The Pascal's hexagon is connected in a profound (although not yet understood way) to alternating sign matrices with various symmetries and as discussed in Appendix A with the solutions of a discrete Hirota's equation.

After this work was almost completed, we learned from Jan de Gier that part of our results were obtained independently by Mitra et al [17]. We have also verified, as discussed in the Appendix, that Pascal's hexagon can be used to obtain properties of the stationary states of stochastic processes related to the periodic TL algebra discussed in [17].

2 Boundary extended Temperley-Lieb algebra

2.1 Definition.

We start with the type A Temperley-Lieb (TL) algebra [18] which as it is well known (see [19]) stands behind the $U_q(sl_2)$ symmetric XXZ spin chain. For the chain of L particles the corresponding TL algebra is generated by the unity and a set of $(L-1)$ elements e_i, $i = 1, \dots (L-1)$, subject to relations

$$e_i e_{i\pm 1} e_i = e_i \ , \qquad e_i^2 = (q + q^{-1})\, e_i \ , \tag{2.1}$$

$$e_i e_j = e_j e_i \ , \qquad \forall\ i, j : |i - j| > 1 \ . \tag{2.2}$$

Here parameter $q \in \mathbb{C}\backslash\{0\}$ of the algebra is related to the anisotropy parameter $\Delta = -(q + q^{-1})/2$ of the spin chain.

A boundary extension of this algebra is achieved by adding two more generators f_0 and f_L together with the relations

$$e_1 f_0 e_1 = e_1 \ , \qquad e_j f_0 = f_0 e_j \ , \quad \forall\ j > 1, \tag{2.3}$$

$$e_{L-1} f_L e_{L-1} = e_{L-1} \ , \qquad e_j f_L = f_L e_j \ , \quad \forall\ j < L-1. \tag{2.4}$$

$$f_0^2 = a\, f_0 \ , \qquad f_L^2 = \bar{a}\, f_L \ , \qquad f_0 f_L = f_L f_0 \ , \tag{2.5}$$

where $a, \bar{a} \in \mathbb{C}$. The algebra with one boundary element (either f_0, or f_L) called the *blob algebra* was analyzed in [14, 15]. The extension of the TL algebra with the two boundary generators was introduced in [11]. Unlike TL and blob algebras it is infinite dimensional and we are going to further extract its finite dimensional quotient. To this end we consider a pair of unnormalized projectors X_L and Y_L. They are defined differently depending on a parity of L

$$\begin{aligned} &\text{for } L \text{ even:} \quad X_L := \prod_{k=0}^{L/2-1} e_{2k+1} , \qquad Y_L := f_0 \prod_{k=1}^{L/2-1} e_{2k}\ f_L ; \\ &\text{for } L \text{ odd:} \quad X_L := f_0 \prod_{k=1}^{(L-1)/2} e_{2k} , \qquad Y_L := \prod_{k=0}^{(L-3)/2} e_{2k+1}\ f_L . \end{aligned} \tag{2.6}$$

In terms of these projectors reduction conditions read

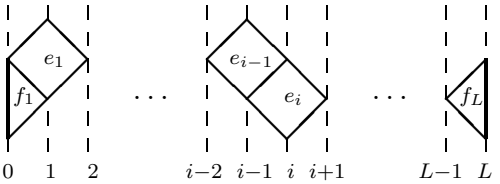
$$X_L Y_L X_L = b\ X_L , \quad Y_L X_L Y_L = b\ Y_L . \tag{2.7}$$

The resulting quotient algebra is that one we shall further call the *boundary extended TL algebra*. It is finite dimensional[3] and it depends on four parameters q, a, $\bar{a}$ and $b \in \mathbb{C}$.

2.2 Graphical presentation.

There are at least two ways in which the boundary extended TL algebra can be visualized. First one is a straightforward generalization of the diagrammatic realization of the blob algebra presented in [14]. For this one uses familiar "lines and loops" diagrams for the TL generators e_i and realizes the boundary generators f_0 and f_L as two different blobs lying, respectively, on the leftmost and the rightmost lines of the diagram (see [14]). Equivalently, one can draw boundary generator f_0 (f_L) as a half-loop connecting the leftmost (rightmost) line to the boundary (see [11, 17]).

The second way which we are using throughout this paper is the one suitable for modelling of growing interfaces (see [12]). One draws the TL generator e_i as a tile whose diagonal is lying on a vertical line with coordinate i and whose left and right vertices are placed, respectively, on vertical lines with coordinates $i-1$ and $i+1$. The boundary generators f_0 and f_L are drawn as half-tiles with their longest sides lying on vertical lines with coordinates 0 and L, respectively (see Figure below).



(2.8)

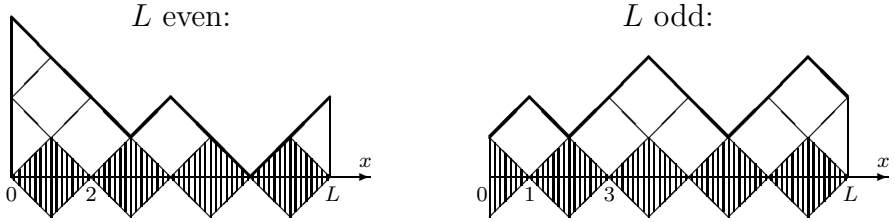
[3]Dimensions of the boundary extended TL algebras are calculated in an Appendix to [20].

The (half-)tiles can freely move along vertical axes unless they meet their neighbors. Assuming attraction forces acting among the (half-)tiles one represents word in the algebra as a collection of dense polygons built from the (half-)tiles and satisfying following conditions. All polygons are placed between vertical lines with coordinates 0 and L and no vertical line lying between these two boundary verticals crosses the borders of (one or several) polygons in more then two points.

2.3 The ideal $\mathcal{I}_L$.

Of our main interest is the left ideal in the boundary extended TL algebra generated by X_L[4]. We denote this ideal as $\mathcal{I}_L$.

Consider graphical realization of a typical word in the ideal. As we have different definitions of X_L depending on a parity of L, separate pictures for the cases of L even and L odd are given below.



(2.9)

Here we adopt a convention that multiplication from the left by elements e_i, f_0, or f_L amounts graphically to dropping their respective (half-)tiles up-down. Components of X_L are shown hatched on the pictures.

As it is obvious from pictures (2.9) each word w in the ideal $\mathcal{I}_L$ is uniquely defined by a shape of the upper border $h(w|x)$, $0 \le x \le L$, of its corresponding polygon (drawn in bold lines on the pictures). In turn, the border line is suitably encoded by its values at the integer points $h(w|i) := h_i(w)$. $i = 0, 1, \ldots, L$. Assuming the height of the tile (= the length of its diagonal) equals 2 and taking the middle line of the bottom row of tiles as a reference axe one gets following prescriptions for a set of $\{h_i\}_{i=0,1,\ldots,L}$

$$
\begin{aligned}
&a)\quad h_{i+1} - h_i = \pm 1 \quad \textit{and} \quad h_i \ge 0\,,\ \forall\, i\,;\\
&b)\quad h_L \textit{ is an even integer;}\\
&c)\quad \textit{there exists } i \textit{ such that } \ h_i \in \{0, 1\}\,.
\end{aligned}
\tag{2.10}
$$

Here prescription b) results from our choice of X_L as an ideal generating element. With the choice of Y_L one would constrain h_0 to be even. Prescription c) arises from the reduction conditions (2.7).

[4]Note that in case $b \neq 0$ the element Y_L generates an isomorphic ideal.

In Ref.[21] a set of data $\{h_i\}_{i=0,1,\ldots,L}$ satisfying conditions (2.10) is named an *Anchored Cross path*, L is called a *length* of the path. Anchored Cross paths of length L label effectively words in the ideal $\mathcal{I}_L$. There are 2^L different Anchored Cross paths of length L (for the proof c.f. Appendix of Ref.[20]) and thus, $\dim \mathcal{I}_L = 2^L$. It is remarkable that the dimension of $\mathcal{I}_L$ coincides with the number of states of the chain of L spin=1/2 particles. This is not just a coincidence and the ideal $\mathcal{I}_L$ can be used for representation of an open XXZ chain of L spin=1/2 particles (see [16]).

In considerations below we will use besides the set of Anchored Cross paths a pair of its subsets (or, equivalently, two subspaces in the ideal $\mathcal{I}_L$). Their definitions are given below.

Ballot paths are the paths (2.10) with fixed endpoint $h_L = 0$. Their total number is $\binom{L}{[L/2]}$, where $[x]$ is an integer part of x. Examples of Ballot paths are shown on pictures a), b) and c) on Fig.1 on page 7. Paths shown on pictures d) and e) are not the Ballot paths.

Dyck paths are usually defined for L even and they are fixed at both ends as $h_0 = h_L = 0$. For $L = 2p$ one has $C_p := \frac{1}{p+1}\binom{2p}{p}$ Dyck paths which is the p-th Catalan number. For L odd close relatives of Dyck paths are those whose endpoints are fixed as $h_0 = 1$, $h_L = 0$. These paths are in one to one correspondence with the Dyck paths of length $L+1$ and later on we will also refer them as Dyck paths. Among the paths shown on Fig. 2 on page 8 cases a), b) and c) are the Dyck paths, while cases d), e), f) are not.

3 Raise and Peel Models with different boundary terms.

3.1 The models definition.

First, we describe the models algebraically and then, we discuss their physical interpretation.

By definition, the ideal $\mathcal{I}_L$ forms left representation space of the boundary extended TL algebra. Consider on this space a dynamical process

$$\frac{d}{dt}\,|p_L(t)\rangle \;=\; -\,H_L\,|p_L(t)\rangle\,, \tag{3.1}$$

$$H_L \;:=\; \sum_{i=1}^{l-1}(1-e_i) + c(1-f_0) + \bar{c}(1-f_L)\,, \tag{3.2}$$

defining an evolution of element $|p_L(t)\rangle \in \mathcal{I}_L$. Here H_L, the Hamiltonian of the process contains two numeric parameters — c and $\bar{c}$, while the process itself depends also on four parameters of the algebra — q, a, $\bar{a}$ and b (see Eqs. (2.1) – (2.5) and (2.7)). We are interested in case where the boundary extended TL algebra becomes semigroup (that is, all the nonvanishing structure constants of the algebra are units) and so we fix algebra parameters as

$$q = exp(i\pi/3)\;(\Rightarrow q + q^{-1} = 1)\,, \quad a = \bar{a} = b = 1\,. \tag{3.3}$$

In this case the Hamiltonian (3.2) becomes an intensity matrix and the process (3.1) can be given a stochastic interpretation (see, e.g., [10]). Expanding element $|p_L(t)\rangle$ into linear

combination of words of the ideal

$$|p_L(t)\rangle = \sum_{w\in\mathcal{I}_L} p_L(w|t)\, w$$

one treats coefficients $p_L(w|t)$ as unnormalized probabilities to find the stochastic system in configuration w at time t.

In this paper we consider stochastic processes (3.1) corresponding to three particular choises of parameters c and $\bar{c}$ of the Hamiltonian (3.2). We call them models A, B, and C,

$$\text{model A: } c=\bar{c}=0\,; \qquad \text{model B: } c=1\,,\ \bar{c}=0\,; \qquad \text{model C: } c=\bar{c}=1\,. \tag{3.4}$$

In cases A and B the Hamiltonian acts invariantly on the subspaces of $\mathcal{I}_L$ spanned, respectively, by all Dyck and Ballot paths. Therefore we shall treat models A/B on their respective irreducible spaces of Dyck/Ballot paths.

Now let us discuss physical interpretation of the models. We consider three processes of growth of a film of tiles which are deposited on a one-dimensional substrate of size L.

As a substrate in all cases we choose profiles which are shown hatched on pictures (2.9). A rarefied gas above the substrate contains tiles and (possibly) half-tiles. They are moving along integer vertical lines as illustrated on picture (2.8) and upon hitting the substrate they can be absorbed and form interface configurations as shown on picture (2.9). Depending on a composition of the gas one distinguishes three cases

model A: the gas contains tiles moving along lines with coordinates $i=1,2,\ldots,L-1$; possible interface configurations are given by Dyck paths;

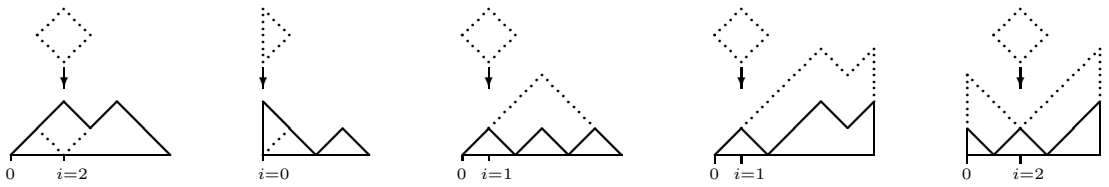
model B: the gas contains all the tiles and the half-tile moving along 0-th line; possible interface configurations are the Ballot paths;

model C: the gas contains all the tiles and the half-tiles on both left and right boundaries; possible interface configurations are the Anchored Cross paths.

To determine evolution rules in the models we use the graphical presentation of the boundary extended TL algebra. We remind that in this presentation the substrate of size L corresponds to the unnormalized projector X_L; interface configurations correspond to words in the ideal $\mathcal{I}_L$; the (half-)tile on i-th vertical line is an equivalent of the algebra generator e_i (f_0/f_L for $i=0/L$); hitting the interface by (half-)tiles amounts to left multiplication by e_i (f_0, f_L) in the ideal. With these identifications equation (3.1) defines following evolution rules.

During an infinitesimal time interval dt a single event may happen with equal probability rate at any integer point of the interface. The following events are possible.

a) At a local minimum point i (that is, if $h_i < h_{i\pm1}$) the interface either absorbs (half-)tile ($h_i \mapsto h_{i+2}$) with probability dt or it reflects (half-)tile (h_i stays unchanged) with probability $1-dt$. For the model C there is an exception from this rule described in item d).



a) b) c) d) e)

Figure 1: The interface profile before event and the (half-)tiles hitting the interface are drawn in dashed lines. The interface profile after the event is drown in permanent line. Pictures a) and b) illustrate absorption, respectively, in a bulk and at the boundary of the interface. Pictures c) and d) are examples of avalanches, respectively, in the bulk (number of desorbed tiles $n_d = 3$, size of a substrate $L = 6$) and near the boundary ($n_d = 5$, $L = 6$). Picture e) shows the total avalanche ($n_d = L = 5$).

b) At a local maximum point i (that is, if $h_i > h_{i\pm1}$) the interface always reflects (half-)tiles and stays unchanged.

c) At a bulk slope point i (that is, $0 < i < L$ and either $h_{i-1} < h_i < h_{i+1}$, or $h_{i-1} > h_i > h_{i+1}$) dropping a tile leads with probability dt to a nonlocal desorption event called avalanche. To describe the avalanche one determines integer k such that for all integers j standing between i and k inequality $h_j > h_i$ holds and either $h_k = h_i$, or k runs out the interval $[0, L]$, i.e., k equals $L + 1$, or -1. The avalanche causes desorption of one tile at each point j between i and k, that is $h_j \mapsto h_j - 2$. The avalanche size (a number of the desorbed (half-)tiles) $n_d = |i - k| - 1$, $1 \le n_d \le L - 1$, measures non-locality of the event.

With probability $1 - dt$ the tile is reflected and the interface stays unchanged.

d) In the model C at a global minimum point i such that $h_i = 1$ and $h_j > h_i\,,\ \forall\ j \neq i\,,$ dropping (half-)tile with probability dt causes total avalanche of a size $n_d = L$ that is, $h_j \mapsto h_j - 2\,,\ \forall\ j \neq i$. Again, with probability $1 - dt$ the (half-)tile is reflected and the interface stays unchanged.

Typical absorption and desorption events are illustrated on Figure 1.

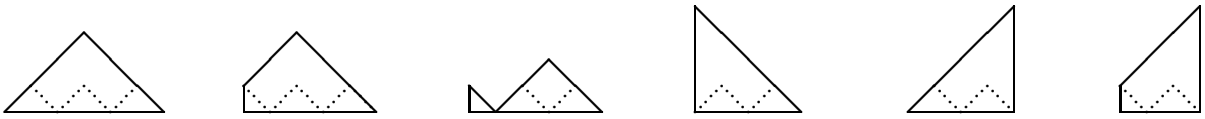
For the model A the evolution rules described here were formulated in Ref. [12]. This stochastic process was named *raise and peel model* (RPM) there. Models B and C are versions of the RPM supplied with additional boundary terms.

3.2 Stationary states: largest and smallest components and normalization factors.

From now on we will study stationary states of the stochastic processes (3.1)–(3.4), i.e. solutions of equation

$$H_L|p_L\rangle \;=\; 0\,. \tag{3.5}$$

Note that the intensity property of matrix H_L guarantees an existence of at least one non-trivial solution of equation (3.5).



a) b) c) d) e) f)

Figure 2: For the model A the minimal possible coefficient 1 in null eigenvector stands for pyramid type configuration a) for L even and for configurations b) and c) for L odd. For the model B half-pyramid configurations d) has coefficient 1 both for L even and L odd. For the model C the minimal coefficient $m_L^{(c)}$ appears again for configurations d) and for e)/f) in case of L even/odd. Dashed lines show the substrate in each case.

Below we present results of a numeric investigation of the stationary states of three versions of RPM. Calculations were carried out with the use of REDUCE program for the system's size up to $L = 13/11/10$ for the models A/B/C, respectively. In all three cases the RPM has a unique stationary state.

Denote components of $|p_L\rangle$ (3.5) in the models A, B and C as $p_L^{(a)}(w)$, $p_L^{(b)}(w)$ and $p_L^{(c)}(w)$, respectively. Here argument w labels in each case relevant interface configurations: those are the sets of Dyck paths $\{w\}_{Dyck}$ in the model A, Ballot paths $\{w\}_{Ballot}$ in the model B and Anchored Cross paths $\{w\}_{ACross}$ in the model C. Due to intensity property of the Hamiltonian one always can choose null eigenvectors $|p_L\rangle$ in such a way that all their components are nonnegative real (see [22]), thus, making the probabilistic interpretation consistent. Moreover, it turns out that no one of coefficients $p_L^{(*)}(w)$ vanishes. So, we can normalize them to be mutually primitive positive integers. Denote their smallest and largest components as

$$m_L^{(*)} := \min_{\{w\}_*}\{p_L^{(*)}(w)\}\,, \qquad M_L^{(*)} := \max_{\{w\}_*}\{p_L^{(*)}(w)\}\,. \tag{3.6}$$

It turns out that $m_L^{(a)} = m_L^{(b)} = 1$, but $m_L^{(c)} \neq 1$. The corresponding interface configurations are shown on Fig.(2).

Denote total normalization factors of the stationary probability distributions as

$$S_L^{(*)} := \sum_{\{w\}_*} p_L^{(*)}(w)\,. \tag{3.7}$$

In the table below we collect values of $S_L^{(*)}$ and $m_L^{(c)}$ for $L \leq 11$

L	1	2	3	4	5	6	7	8	9	10	11
$S_L^{(a)}$	1	1	2	3	11	26	170	646	7429	45885	920460
$S_L^{(b)}$	1	2	6	33	286	4420	109820	4799134	340879665	42235307100	8564558139000
$S_L^{(c)}$	2	6	66	858	48620	1427660	47991340	11589908610	13642004193300	1139086232487000	
$m_L^{(c)}$	1	1	2	3	11	13	10	34	323	133	

(3.8)

The table illustrates clearly the following three conjectures. These conjectures were found also in [2, 17].

Conjecture 1. *Let A_n^V (resp., A_n^{VH}) denote a number of vertically symmetric (resp., vertically and horizontally symmetric) alternating sign matrices of a size $n \times n$* [5]*. Then*

$$S_{2p}^{(a)} = A_{2p+1}^V := (-3)^{p^2} \prod_{\substack{1 \le i \le p \\ 1 \le j \le 2p+1}} \frac{6i-3j+1}{2i-j+2p+1} \ , \qquad S_L^{(b)} = A_{2L+3}^{VH} \ . \tag{3.9}$$

Conjecture 2. *Looking at numbers standing in down-up diagonals of the table one observes equalities*

$$S_L^{(b)} \ = \ S_L^{(a)} \ S_{L+1}^{(a)} \ , \tag{3.10}$$

$$S_L^{(c)} \ = \ m_L^{(c)} S_{L+1}^{(b)} \ . \tag{3.11}$$

The first equality (3.10) allows one to get two expressions for $S_{2p-1}^{(a)}$ [6]

$$S_{2p-1}^{(a)} \ = \ A_{4p-1}^{VH}/A_{2p-1}^V \ = \ A_{4p+1}^{VH}/A_{2p+1}^V := \prod_{0 \le i \le p-1} \frac{(3i+1)(6i)!(2i)!}{(4i)!(4i+1)!} \, . \tag{3.12}$$

Their consistency, in turn, is based on relations conjectured in [23]

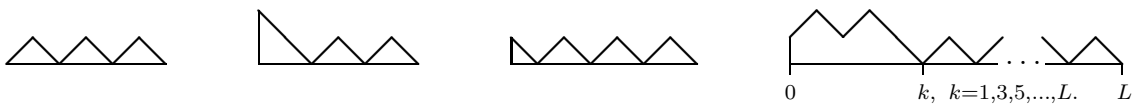
$$A_{4p+1}^{VH}/A_{4p-1}^{VH} \ = \ A_{2p+1}^V/A_{2p-1}^V \ = \ \frac{(3p-1)\binom{6p-3}{2p-1}}{(4p-1)\binom{4p-2}{2p-1}} \, . \tag{3.13}$$

The second equality (3.11) relates quantities $S_L^{(c)}$ and $m_L^{(c)}$. Looking at the table (3.8) one can also assume that $m_L^{(c)}$ are divisors of $S_L^{(a)}$. A formula for $m_L^{(c)}$ refining this observation is guessed in [17] (see Eqs.(32), (33) there)

$$m_L^{(c)} = \text{Numerator of } \left(\frac{S_L^{(a)}}{S_{L+2}^{(a)}} \right) \ . \tag{3.14}$$

[5] On enumeration of various symmetry classes of alternating sign matrices see [23, 24]

[6] Note that $S_{2p-1}^{(a)}$ is just the number of cyclically symmetric transpose complement plane partitions in a $(2p)^3$ box (see, e.g., [25], p.199). It is usually denoted as $N_S(2p)$.



a) b) c) d)

Figure 3: In the model A the maximal coefficient in null eigenvector stands for configuration a) for L even and for configurations d) for L odd. In the model B configurations a) and b) enter the null eigenvector with the maximal coefficient if L is even and configuration c) corresponds to maximal coefficient if L is odd.

Remark. At this point one may propose another reasonable normalization for the stationary state in the model C. Denoting components of the stationary state in this new normalization as $\{\widetilde{p}_L^{(c)}\}$ one may fix normalization demanding that

$$\widetilde{m}_L^{(c)} := \min_{\{w\}_{ACross}} \{\widetilde{p}_L^{(c)}(w)\} = S_L^{(a)}\,, \tag{3.15}$$

Certainly, the initial normalization is a more economic one and thus it is better suited for calculations. However, normalization (3.15) has an advantage in interpreting results. E.g., formula for the total normalization factors in this case looks as

$$\widetilde{S}_L^{(c)} \;=\; S_L^{(a)} S_{L+1}^{(b)} \;=\; S_L^{(b)} S_{L+2}^{(a)} \;=\; S_L^{(a)} S_{L+1}^{(a)} S_{L+2}^{(a)}\,, \tag{3.16}$$

which is much more in the spirit of eq.(3.10) then the formula (3.11). We decide to keep initial 'economic' normalization throughout the text and to comment on the second normalization when presenting results.

The last conjecture of this section describes the largest components of the stationary states in the models A and B. Analogous results for the model C are given in conjecture 13.

Conjecture 3. *The maximal coefficient $M_L^{(a)}$ appear in the set $\{p_L^{(a)}\}$ with multiplicity 1 for L even and $(L-1)/2$ for L odd. The maximal coefficient $M_L^{(b)}$ appear in the set $\{p_L^{(b)}\}$ with multiplicity 2 for L even and 1 for L odd. Their corresponding interface configurations are shown on Fig.(3) and values of the maximal coefficients are given by formulas*

$$M_L^{(a)} \;=\; S_{L-1}^{(a)}\,, \tag{3.17}$$

$$M_{L=2p}^{(b)} \;=\; (S_L^{(a)})^2\,, \quad M_{L=2p+1}^{(b)} \;=\; S_{L-1}^{(a)} S_{L+1}^{(a)}\,. \tag{3.18}$$

3.3 Model A: detailed distributions and Pascal's hexagon relation

Let us first introduce more notation.

An integer point i of an interface configuration $\{h_k\}_{k=0,\ldots,L}$ such that $0 < i < L$ for the model A; $0 \le i < L$ for the model B; or, $0 \le i \le L$ for the model C, is called an *N-contact* if $h_i = N$ and $h_{i\pm1} = N+1$. The contact points are local minima of the interface at which it can absorb (half-)tiles. For instance, the interface shown on picture d) of Fig.(3) has only one 1-contact $i = 2$ in case A, but it has two 1-contacts $i = 0, 2$ in cases B, or C. In all cases

it has 0-contacts at points $k, k+2, \ldots L-2$ and additionally it has 0-contact at point L in case C.

For either of the families of Dyck, Ballot, or Anchored Cross paths we denote $\{w\}_*^N$ (here $*$ stands for an appropriate family name) the subsets of all interface configurations which have no p-contacts with $p < N$. These are the configurations whose global minimum (excluding points 0 and L for the model A, or point L for the model B) is higher or equal to N. Obviously, one has $\{w\}_*^0 \equiv \{w\}_*$ and $\{w\}_*^{N+1} \subset \{w\}_*^N$. We shall stress that there is no strict correlation between the subsets $\{w\}_*^N$ corresponding to different sets of paths. For example, for any N

$$\{w\}_{Dyck}^N \subset \{w\}_{Ballot}^k\,, \qquad \{w\}_{Dyck}^N \cap \{w\}_{Ballot}^{k+1} = \emptyset\,,$$

where $k = 0/1$ for L even/odd. This is because the left boundary point $h_0 = 0,$ or 1 of a Dyck path is treated as 0-, or 1-contact point in a family of Ballot paths.

Considering the subsets $\{w\}_*^N$ proves to be useful for analysis of the raise and peel model in cases A and B. Here label N spans integers from 0 to $[(L-1)/2]$ in case A and from 0 to $(L-1)$ in case B.[7] The subset with highest possible N in both models A and B contains only element which is drawn on Fig.(2), pictures a)/b) and d), respectively. As it was mentioned before, this element enters the stationary state with a minimal coefficient 1. In the sequel we determine detailed distributions $S_{L,N}^{(*)}$ and detailed maxima $M_{L,N}^{(*)}$ for each of the subsets $\{w\}_*^N$

$$S_{L,N}^{(*)} := \sum_{\{w\}_*^N} p_L^{(*)}(w)\,, \qquad M_{L,N}^{(*)} := \max_{\{w\}_*^N}\{p_L^{(*)}(w)\}\,. \tag{3.19}$$

In this section we concentrate on studying the model A. The table below contains values of $S_{L,N}^{(a)}$ for L up to 13.

$L\backslash N$	−1	0	1	2	3	4	5	6
1		1						
2	1		1					
3		2		1				
4	3		3		1			
5		11		4		1		
6	26		26		5		1	
7		170		50		6		1
8	646		646		85		7		1
9		7429		1862		133		8		1	
10	45885		45885		4508		196		9		1	
11		920460		202860		9660		276		10		1	
12	9304650		9304650		720360		18900		375		11		1	
13		323801820		64080720		2184570		34452		495		12		1

(3.20)

[7] By contrast, for the model C label N can take only two values — 0 and 1.

For later convenience we add to the table a column for $N=-1$ setting $S^{(a)}_{L=2p,N=-1} := S^{(a)}_{L=2p,N=0}$. We also align data corresponding to even, or odd values of L leftwards, or rightwards in the columns, correspondingly. The numbers $S^{(a)}_{L,N=0} \equiv S^{(a)}_{L}$ were already listed in table (3.8).

It is helpful to look at the up-down diagonals in this table. The rightmost diagonal contains units only. the next one contains numbers $(L-1)$. For numbers staying in diagonals from third to seventh one finds expressions

$$\frac{(L-2)(L-3)\cdot(2L+1)}{2\cdot 3}\,, \tag{3.21}$$

$$\frac{(L-2)(L-3)(L-4)(L-5)\cdot(2L+1)(2L+3)}{2^2\cdot 3^2\cdot 5}\,, \tag{3.22}$$

$$\frac{(L-3)(L-4)^2(L-5)(L-6)(L-7)\cdot(2L-1)(2L+1)(2L+3)(2L+5)}{2^4\cdot 3^3\cdot 5^2\cdot 7}\,, \tag{3.23}$$

$$\frac{(L-3)(L-4)(L-5)^2(L-6)^2(L-7)(L-8)(L-9)\cdot(2L-1)(2L+1)^2(2L+3)(2L+5)(2L+7)}{2^6\cdot 3^4\cdot 5^3\cdot 7^2\cdot 9}\,, \tag{3.24}$$

$$\frac{(L-4)(L-5)^2(L-6)^2(L-7)^2(L-8)^2(L-9)(L-10)(L-11)\cdot(2L-3)(2L-1)(2L+1)^2(2L+3)^2(2L+5)(2L+7)(2L+9)}{2^9\cdot 3^5\cdot 5^4\cdot 7^3\cdot 9^2\cdot 11}\,. \tag{3.25}$$

With these data one can guess general formula for $S^{(a)}_{L,N}$.

Conjecture 4 (Model A: detailed distributions). *Denote $n := [\frac{L-1}{2}] - N$. Integer n starts from 0 and labels leftwards the up-down diagonals in the table (3.20). One has*

$$S^{(a)}_{L,N} \;=\; 2^{-[n^2/4]} \prod_{p=1}^{n} \frac{1}{(2p-1)!!} \prod_{p=0}^{[\frac{n-1}{3}]} \frac{(L-[\frac{n+p}{2}]-p-1)!}{(L-2n+3p)!} \prod_{p=0}^{[\frac{n-2}{3}]} \frac{(2L+2n-6p-3)!!}{(2L-2[\frac{n+p}{2}]+4p+1)!!} \tag{3.26}$$

The same sequence was guessed in [17] [8]. Our notation is related to that used in [17] as $S^{(a)}_{L,N=[(L-1)/2]-n} \equiv R(n+1, L+1)$ (see eq.(17) there).

As it is explained, e.g., in [11, 17] the numbers given by formula (3.26) appear in counting elements of certain families of vertically symmetric alternating sign matrices. It is not however clear how one can characterize these families of ASMs. The table (3.20) suggests another combinatorial interpretation of integers $S^{(a)}_{L,N}$.

Pascal's hexagon relations. *The numbers in sequence $S^{(a)}_{L,N}$ (3.26) satisfy equalities*

$$S^{(a)}_{L-1,N} S^{(a)}_{L+1,N+1} + S^{(a)}_{L,N-1} S^{(a)}_{L,N+1} \;=\; S^{(a)}_{L-1,N+1} S^{(a)}_{L+1,N}\,, \quad \textit{if } L \textit{ is even}\,, \tag{3.27}$$

[8] For a particular case $L=2p$, $N=1$ distributions $S^{(a)}_{2p,1}$ coincide with $P_p(1)$, where $P_p(k)$ is the unnormalized probability to have k clusters in the stationary state (see [12]). An expression for $P_p(k)$ is given in Conjecture 3 in [11].



a) b)

Figure 4: In the model A configurations a)/b) of a size $L = 9/10$ have no 0- and 1-contacts. Thus, they belong to subset $\{w\}^{N=2}_{Dyck}$. In this subset among all the configurations of a fixed size $L = 9/10$ they have maximal possible number $n = 2$ of 2-contacts and in accordance with the statement of Conjecture 5 they enter the stationary state with a maximal coefficients $M^{(a)}_{L=9/10,N=2}$.

$$S^{(a)}_{L-1,N}S^{(a)}_{L+1,N+1} + S^{(a)}_{L,N}S^{(a)}_{L,N+2} \;=\; S^{(a)}_{L-1,N+1}S^{(a)}_{L+1,N}\,, \quad \textit{if } L \textit{ is odd}. \tag{3.28}$$

Substituting label N by $n := ([\frac{L-1}{2}] - N)$ in the notation $S^{(a)}_{L,N}$ one can uniformly write relations (3.27), (3.28) as

$$S^{(a)}_{L-1,n}S^{(a)}_{L+1,n} + S^{(a)}_{L,n-1}S^{(a)}_{L,n+1} \;=\; S^{(a)}_{L-1,n-1}S^{(a)}_{L+1,n+1}\,. \tag{3.29}$$

In table (3.20) numbers participating in eq.(3.29) form a hexagonal structure. One such hexagon is drawn in the table. The components of each square monomial in (3.29) occupy opposite vertices of the hexagon. Relation (3.29) thus looks as a sophisticated variant of Pascal's triangle relation, wherefrom our notation follows.

Like in Pascal's triangle case relations (3.29) can be used to reconstruct all numbers $S^{(a)}_{L,n}$ provided some, say boundary, part of them are fixed. For certain boundary data the numbers $S^{(a)}_{L,n}$ turn out to be integers and one recognizes among them the numbers of vertically symmetric and half turn symmetric alternating sign matrices, A^{V}_{2n+1} and A^{HT}_{n}, whereas the total number of ASMs A_n, and the number of vertically and horizontally symmetric ASMs A^{VH}_{n} appear in combinations. A brief discussion of this subject is presented in the Appendix.

We finish the section with observations of detailed maxima and of symmetry properties of the stationary distribution.

Conjecture 5 (Model A: detailed maxima). *In the stationary state of the model A maximal coefficient $M^{(a)}_{L,N}$ in the subset $\{w\}^{N}_{Dyck}$ stands for configuration with a maximal possible number $([(L-1)/2] - N)$ of N-contacts (see explanations on Fig.(4)). It is given by formula*

$$M^{(a)}_{L,N} \;=\; S^{(a)}_{L-1,N-\epsilon(L)}\,, \tag{3.30}$$

where $\epsilon(L) := \frac{1-(-1)^L}{2}$ is a parity function. [9]

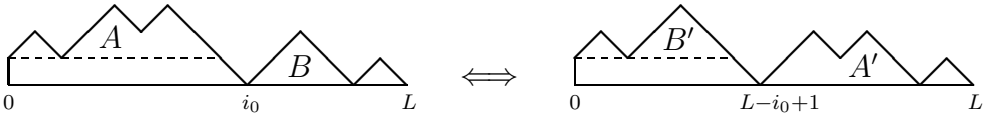
The relation (3.30) was also observed in [17]. Note that in case $N = 0$ and L odd we use in eq.(3.30) an extension of sequence $S^{(a)}_{L,N}$ to case $N = -1$ that we made in table (3.20).

[9] Here and everywhere below in the main text we use definition of $S^{(a)}_{L,N}$ as it is given in eq.(3.26). This notation is natural for the stochastic models we are treating. Different convention about the second index in $S^{(a)}_{L,n}$ is used in eq.(3.29) and in the Appendix. It is more suitable from a mathematical viewpoint.

Note also that equality $M^{(a)}_{L=2p+1,N=0} = M^{(a)}_{L=2p+1,N=1}$ following from (3.30) agrees with the statements made in Conjecture 3 (see Fig.(3), picture d), cases $k = 1$ and $k = L$).

Conjecture 6. *In the model A for any configuration $\{h_i\}$ there exists a configuration $\{h'_i\}$ which appears in the stationary state with the same coefficient. The definition of $\{h'_i\}$ is following*
– for L even, $h'_i := h_{L-i}$;
– for L odd, let i_0 be coordinate of the leftmost 0-contact point in configuration $\{h_i\}$, or $i_0 = L$ if there is no 0-contacts in $\{h_i\}$. Then, $h'_i := h_{L-i} + 1$ for all $i \le L - i_0$, and $h'_i := h_{L-i} - 1$ for all $i > L - i_0$.

For L even the statement of Conjecture 6 is a direct consequence of the left-right symmetry of the Hamiltonian and the configuration space. For L odd the space of the states is no more left-right symmetric, and the symmetry is not an obvious one. Typical pair of symmetric configurations is drawn below (pieces of paths A/B and A'/B' are left-right symmetric).



3.4 Model B: left orbits and factorizations to model A

Again, we start with a few definitions.

Consider a configuration $w = \{h_k\}_{k=0,\dots,L}$ from the set of Anchored Cross paths. For any N-contact point i of the configuration w we construct new configurations $w_l(i)$ and $w_r(i)$ (here value of N is irrelevant)

$$w_l(i) = \{h'_k\}: \qquad h'_k := \begin{cases} h_k + 2 & \text{for} \quad 0 \le k \le i\,, \\ h_k & \text{for} \quad i < k \le L\,, \end{cases} \tag{3.31}$$

$$w_r(i) = \{h''_k\}: \qquad h''_k := \begin{cases} h_k & \text{for} \quad 0 \le k < i\,, \\ h_k + 2 & \text{for} \quad i \le k \le L\,, \end{cases} \tag{3.32}$$

It may happen that either one or both configurations $w_l(i)$ and $w_r(i)$ defined by eqs.(3.31), (3.32) do not satisfy condition c) of the definition (2.10) of Anchored Cross paths. Such configurations $w_l(i)/w_r(i)$ should undergo total avalanche (see the end of Sec. 3.1), i.e., they are to be redefined as

$$\{h'^{/\prime\prime}_k\}_{k=0,\dots,L} \longrightarrow \{h'^{/\prime\prime}_k - 2\}_{k=0,\dots,L}\,, \tag{3.33}$$

Thus defined configurations $w_l(i)$ and $w_r(i)$ are called, respectively, *left and right coverings of the configuration w at the point i*. Below, using the notion of left and right coverings we give an iterative description of left and right orbits of the configuration w.

Let $L(w,N)/R(w,N)$ denote a set of all N-contacts of w which do not occupy right/left boundary point and which are placed to the left/right of any k-contact with $k < N$. First, we

construct left/right coverings $w_l(i)/w_r(j)$ of w at all points $i \in L(w,N)/j \in R(w,N)$. Note that for all coverings $w_l(i)/w_r(j)$ the sets $L(w_l(i),N)/R(w_r(j),N)$ lie strictly inside the set $L(w,N)/R(w,N)$. Next, we construct left/right coverings for all obtained at a first step configurations $w_l(i)/w_r(j)$ at all points from their corresponding sets $L(w_l(i),N)/R(w_r(j),N)$. We repeat the procedure until at some step of iteration there will be no more N-contacts available for generation of new coverings. The set of all thus obtained left/right coverings together with w itself is called *left/right N-orbit of the configuration w* and is denoted as $\mathcal{O}_l(w,N)/\mathcal{O}_r(w,N)$; w is called *generating element* of the orbit. The process of iterative construction of left and right orbits is illustrated on Fig.6, p.30 and Fig.7, p.31, respectively. One can see that the numbers of elements in the orbits $\mathcal{O}_l(w,N)/\mathcal{O}_r(w,N)$ and in the sets $L(w,N)/R(w,N)$ are related as

$$\#\mathcal{O}_l(w,N) \,=\, 2^{\#L(w,N)}\,, \qquad \#\mathcal{O}_r(w,N) \,=\, 2^{\#R(w,N)}\,. \tag{3.34}$$

An N-orbit is called *maximal* if it is not a subset of some bigger N-orbit.

For the family of Ballot paths only the procedure of left covering makes sense and, hence, only the left orbits are defined. In the rest of this section we apply notion of the left orbits to establish detailed relations for the stationary states in case B raise and peel model. The maximal 0- and 1-orbits will be especially important for us. The reasons are following.

The family of Ballot paths splits uniquely into collection of all (mutually nonintersecting) maximal left 0-/1-orbits.

The maximal left 0-orbits of length L are generated by elements

$$w = \{h_k\}_{k=0,\ldots,L}: \quad h_0 = \begin{cases} 0 & \text{for } L \text{ even}, \\ 1 & \text{for } L \text{ odd}. \end{cases} \tag{3.35}$$

The maximal left 1-orbits of length L are generated by elements

$$w = \{h_k\}_{k=0,\ldots,L}: \quad h_0 = \begin{cases} \text{either } 0, \text{ or } 2 & \text{for } L \text{ even}, \\ 1 & \text{for } L \text{ odd}. \end{cases} \tag{3.36}$$

We further observe that sums of the stationary coefficients over maximal left 0- and 1-orbits in case B are related to certain stationary coefficients in case A. These relations generalizing formula (3.10) are presented in

Conjecture 7. *Take any Dyck paths u and v of the lengths L and $(L+1)$, respectively. Denote ${}^*v$ a Ballot path of the length L which is a (left) reduction of the Dyck path v, i.e.,*

$$h_k({}^*v) = h_{k+1}(v)\,, \quad \textit{for all} \;\; k = 0,\ldots,L\,.$$

With these notations one has

$$\textit{for } L \textit{ even:} \qquad \sum_{\nu\in\mathcal{O}_l(u,0)} p_L^{(b)}(\nu) \,=\, S_{L+1}^{(a)}\, p_L^{(a)}(u)\,, \qquad \sum_{\nu\in\mathcal{O}_l({}^*v,1)} p_L^{(b)}(\nu) \,=\, S_L^{(a)}\, p_{L+1}^{(a)}(v)\,, \tag{3.37}$$

$$\textit{for } L \textit{ odd:} \qquad \sum_{\nu\in\mathcal{O}_l(^*v,0)} p_L^{(b)}(\nu) \,=\, S_L^{(a)}\, p_{L+1}^{(a)}(v)\,, \qquad \sum_{\nu\in\mathcal{O}_l(u,1)} p_L^{(b)}(\nu) \,=\, S_{L+1}^{(a)}\, p_L^{(a)}(u)\,. \tag{3.38}$$

Here summation is taken over all elements of the left 0-, or 1-orbits generated by u, or $^*v$ (note that configurations u and $^*v$ span all generating elements described in (3.35), (3.36)).

Combining the last conjecture with conjectures 4–6 from the previous section one can get explicit values for sums over certain 0- and 1-orbits. These results and similar formulas for higher orbits are presented in the next

Conjecture 8. *Let us denote $W(h_0, s) = \{h_k\}_{k=0,\ldots,L}$ a Ballot path of a size L such that for a given left boundary height h_0 it has maximal possible number of s-contact points. We are interested in configurations where s take values between $max\{0, (h_0-1)\}$ and $(\frac{L+h_0}{2}-1)$ (see Fig.(5)).*

One can guess explicit expressions for sums of the coefficients $p_L^{(b)}$ over left h_0- and (h_0-1)-orbits generated by elements $W(h_0, s)$. For even size L parameter h_0 takes on even values from 0 to L and one has relations

$$\begin{aligned} (h_0 = 2m)\textit{-orbits:} \qquad & \sum_{\nu\in\mathcal{O}_l(W(h_0=2m,s),2m)} p_L^{(b)}(\nu) \;=\; S_{L+1,m}^{(a)}\, S_{L-1,s-m}^{(a)}\,, \\ (h_0-1 = 2m-1)\textit{-orbits:} \qquad & \sum_{\nu\in\mathcal{O}_l(W(h_0=2m,s),2m-1)} p_L^{(b)}(\nu) \;=\; S_{L,m-1}^{(a)}\, S_{L,s-m}^{(a)}\,. \end{aligned} \tag{3.39}$$

The last formula is applicable in case $m = 0$, i.e., for (-1)-orbits. In this case all the (-1)-orbits are treated as singlets containing their generating elements only.

For odd size L parameter h_0 takes on odd values from 1 to L and one has relations

$$\begin{aligned} (h_0-1 = 2m)\textit{-orbits:} \qquad & \sum_{\nu\in\mathcal{O}_l(W(h_0=2m+1,s),2m)} p_L^{(b)}(\nu) \;=\; S_{L,m}^{(a)}\, S_{L,s-m}^{(a)}\,, \\ (h_0 = 2m+1)\textit{-orbits:} \qquad & \sum_{\nu\in\mathcal{O}_l(W(h_0=2m+1,s),2m+1)} p_L^{(b)}(\nu) \;=\; S_{L+1,m}^{(a)}\, S_{L-1,s-m-1}^{(a)}\,. \end{aligned} \tag{3.40}$$

This Conjecture is graphically illustrated on Fig.6 on page 30.

Most of the orbits appearing in the left hand sides of relations (3.39) and (3.40) are singlets and doublets. Namely, one has singlet (h_0-1)-orbits in case $s \geq h_0$ and singlet h_0-orbits for $s = h_0 - 1$; one has doublet h_0-orbits in case $s \geq h_0 + 1$. The larger size $2^{\frac{L-h_0}{2}}$-plet h_0- and (h_0-1)-orbits appear, respectively, for $s = h_0$ and $s = h_0 - 1$.

Relations for singlets and doublets provide explicit expressions for a number of stationary state coefficients in the model B. In particular, formulas for (h_0-1)-singlets generated by elements $W(h_0, s)$ with $s \geq h_0$ were observed in [17].

Noticing that two configurations from h_0-doublet generated by $W(h_0, h_0+1)$ correspond to (h_0-1)- and (h_0+2)-singlets generated by $W(h_0, h_0+1)$ and $W(h_0+2, h_0+1)$, respectively,

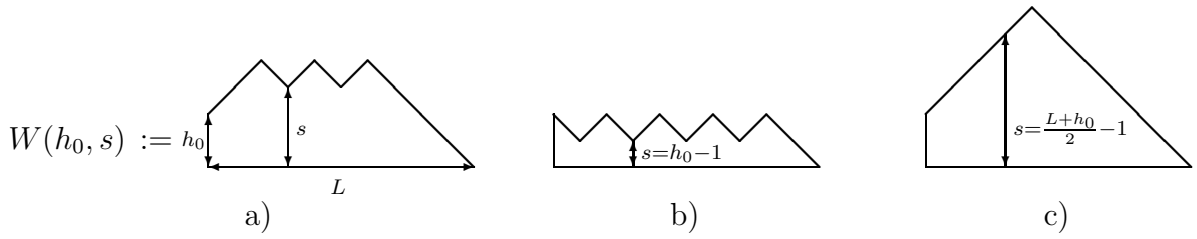


Figure 5: A typical configuration $W(h_0, s)$ is shown on picture a). It is uniquely defined by its size L, its left boundary height h_0 and the height s of its contact points in the bulk. A number of s-contacts in such configuration equals $(\frac{L+h_0}{2} - s - 1)$. Boundary cases with $s = (h_0 - 1)$ and $s = (\frac{L+h_0}{2} - 1)$ are shown, respectively, on pictures b) and c). In the last case one uses parameter s just by analogy, because configuration c) contains 0 number of contacts in the bulk.

one concludes that expressions from the right hand sides of relations (3.39) and (3.40) should comply certain consistency rules. These are just Pascal's hexagon relations (3.27), (3.28) and in this way Pascal's hexagon relations were first time observed.

We finish the section with several observations about detailed normalizations and extremes in the model B.

Conjecture 9 (Model B: detailed distributions I). *For the quantities $S^{(b)}_{L,N}$ introduced in (3.19) one has formulas*

$$\begin{aligned} \textit{for } L \textit{ even:} \qquad S^{(b)}_{L,N} &= S^{(a)}_{L+1,[\frac{N+1}{2}]}\, S^{(a)}_{L,[\frac{N}{2}]}\,, \\ \textit{for } L \textit{ odd:} \qquad S^{(b)}_{L,N} &= S^{(a)}_{L+1,[\frac{N}{2}]}\, S^{(a)}_{L,[\frac{N+1}{2}]}\,. \end{aligned} \tag{3.41}$$

The same formulas for $S^{(b)}_{L,N}$ were observed in [17] (see eq.(48) there).

We remind that label N refers to global minimum of Ballot paths contributing to distribution $S^{(b)}_{L,N}$ (it should be greater or equal to N). N may take all integer values from 0 to L. For $N = 0$ relations (3.41) coincide with eq.(3.10).

One can consider another set of detailed distributions $\Sigma^{(b)}_{L,N,M}$ which count stationary state contributions of all configurations w whose left boundary height is fixed as $h_0(w) = N$ and whose all s-contacts in the bulk satisfy condition $s \geq M$ (i.e., whose global minimum in the bulk is greater or equal to M). For $M \geq N$ all such configurations can be obtained by adding tiles (not half-tiles!) to the configuration $W(h_0 = N, s = M)$ drawn on Fig.5 a).

Note that (in contrast to the case of $S^{(b)}_{L,N}$) for distributions $\Sigma^{(b)}_{L,N,M}$ label N may take only integer values between zero and L which are of the same parity as L.

Conjecture 10 (Model B: detailed distributions II). *In case $M \geq N$ quantities $\Sigma^{(b)}_{L,N,M}$ are given by formula*

$$\Sigma^{(b)}_{L,N,M} = S^{(a)}_{L+1,\, M-[\frac{N-1}{2}]}\, S^{(a)}_{L,[\frac{N-1}{2}]}\,. \tag{3.42}$$

We were unable to find similar expressions in case $M < N$.

The right hand sides of eqs.(3.41) and (3.42) contain the same square combination $S^{(a)}_{L+1,X}S^{(a)}_{L,Y}$ but for indices X, Y taking values in adjacent domains. Hence, formally speaking one can view distributions $S^{(b)}_{L,N-1}$ and $S^{(b)}_{L,N-2}$ as extrapolations of distribution $\Sigma^{(b)}_{L,N,M}$ to cases $M = N-1$ and $M = N-2$, respectively. However, we don't know any non-formal explanation to this fact.

Conjecture 11 (Model B: detailed extremes). *Among elements of the set $\{w\}^{N}_{Ballot}$ configuration with maximal possible number $[\frac{L-N}{2}]$ of N-contacts enters the stationary state with the maximal coefficient $M^{(b)}_{L,N}$ (see def.(3.19)). All such configurations are generating elements $W(h_0, s = h_0-1)$, or $W(h_0, s = h_0)$, respectively, for h_0-, or (h_0-1)-singlet orbits. Hence, expressions for maxima $M^{(b)}_{L,N}$ are particular cases of formulas (3.39),(3.40) (index s there corresponds to N in the notation for detailed maxima). They are*

$$\textit{for } L \textit{ even:} \qquad \begin{aligned} M^{(b)}_{L,N=2m} &= S^{(a)}_{L,m-1}\, S^{(a)}_{L,m}\,, \\ M^{(b)}_{L,N=2m+1} &= S^{(a)}_{L+1,m+1}\, S^{(a)}_{L-1,m}\,; \end{aligned} \tag{3.43}$$

$$\textit{for } L \textit{ odd:} \qquad \begin{aligned} M^{(b)}_{L,N=2m} &= S^{(a)}_{L+1,m}\, S^{(a)}_{L-1,m-1}\,, \\ M^{(b)}_{L,N=2m+1} &= S^{(a)}_{L,m}\, S^{(a)}_{L,m+1}\,. \end{aligned} \tag{3.44}$$

In case of L even and $N = 0$ there is one more configuration $w = \{h_0 = 2, h_i = \epsilon(i)\}$ (see Fig.3 b) on p.10) which enters the stationary state with the same maximal coefficient.

Among all Ballot paths with the same left boundary height h_0 configuration which have no any contact points in the bulk enters the stationary state with a minimal coefficient $m^{(b)}_{L,h_0}$. All such configurations are generating elements $W(h_0, s = \frac{L+h_0}{2}-1)$ of (h_0-1)-singlet orbits. So, expressions for $m^{(b)}_{L,h_0}$ can be found among formulas eqs.(3.39), (3.40). They are

$$m^{(b)}_{L,h_0} \;=\; S^{(a)}_{L,\,[\frac{h_0-1}{2}]}\,. \tag{3.45}$$

3.5 Model C: right orbits and factorizations to model B

In this section we consider right 0- and 1-orbits in a family of Anchored Cross paths and describe corresponding stationary distributions for the model C. Our key observations are following.

The family of Anchored Cross paths splits uniquely into collection of all (mutually non-intersecting) maximal right 0-/1-orbits.

The maximal right 0-orbits of length L are generated by elements

$$w = \{h_k\}_{k=0,\ldots,L}: \quad h_L = 0\,. \tag{3.46}$$

The maximal right 1-orbits of length L are generated by elements

$$w = \{h_k\}_{k=0,\ldots,L}: \qquad \text{either } h_L = 0, \text{ or } h_L = 2 \text{ and } \min_{0\le i\le L} h_i = 1 \text{ (i.e., } \neq 0)\,. \tag{3.47}$$

We further observe that sums of the stationary coefficients over maximal right 0- and 1-orbits in case C are related to certain stationary coefficients in case B. These relations generalizing formula (3.11) are given in

Conjecture 12. *Take any Ballot paths u and v of the lengths L and $(L+1)$, respectively. Denote v^* an Anchored Cross path of the length L which is a (right) reduction of the Ballot path v, i.e.,*

$$\text{for all } \; k = 0,\ldots,L, \quad h_k(v^*) = \begin{cases} h_k(v) + 1\,, & \text{if } \min_{k=0}^{L} h_k(v) = 0\,, \\ h_k(v) - 1\,, & \text{otherwise.} \end{cases}$$

With these notations one has

$$\sum_{\nu\in\mathcal{O}_r(u,0)} p_L^{(c)}(\nu) \;=\; \text{Denominator of } \left(\frac{S_L^{(a)}}{S_{L+2}^{(a)}}\right) p_L^{(b)}(u) \;\equiv\; \frac{m_L^{(c)} S_{L+2}^{(a)}}{S_L^{(a)}}\, p_L^{(b)}(u)\,, \tag{3.48}$$

$$\sum_{\nu\in\mathcal{O}_r(v^*,1)} p_L^{(c)}(\nu) \;=\; \text{Numerator of } \left(\frac{S_L^{(a)}}{S_{L+2}^{(a)}}\right) p_{L+1}^{(b)}(v) \;\equiv\; m_L^{(c)}\, p_{L+1}^{(b)}(v)\,. \tag{3.49}$$

Here summation is taken over all elements of the right 0-, or 1-orbits generated by u, or v^* (configurations u and v^* span all generating elements described in (3.46), (3.47)).

This Conjecture is graphically illustrated on Fig.7 on page 31.

Remark 1. In normalization (3.15) relations (3.48) and (3.49) read

$$\sum_{\nu\in\mathcal{O}_r(u,0)} \tilde{p}_L^{(c)}(\nu) \;=\; S_{L+2}^{(a)} p_L^{(b)}(u)\,, \tag{3.50}$$

$$\sum_{\nu\in\mathcal{O}_r(v^*,1)} \tilde{p}_L^{(c)}(\nu) \;=\; S_L^{(a)}\, p_{L+1}^{(b)}(v)\,. \tag{3.51}$$

In this presentation Conjecture 12 looks very much in the spirit of Conjecture 7 and one can be immediately convinced that it refines formula (3.16).

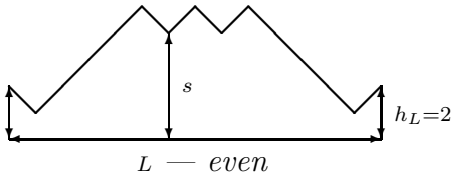
Remark 2. In the model C stationary state obeys mirror symmetry. Namely, any pair of configurations $\{h_k\}$ and $\{h'_k\}$ whose shapes are left-right symmetric, i.e.,

$h'_k = h_{L-k}$ for all k in case of L even;

$$h'_k = \begin{cases} h_{L-k} + 1\,, & \text{if} \quad \min_{i=0}^{L} h_i = 0\,, \\ h_{L-k} - 1\,, & \text{if} \quad \min_{i=0}^{L} h_i = 1\,, \end{cases} \quad \text{for all } k \text{ in case of } L \text{ odd;}$$

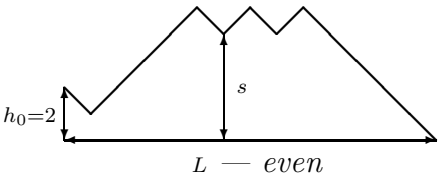
enter the stationary state with the same coefficients. Using this symmetry one can reformulate Conjecture 12 in the language of left orbits.

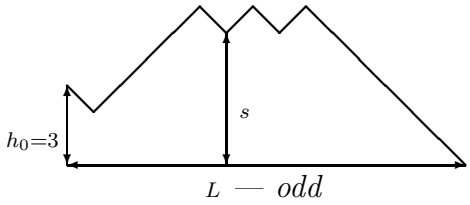
There are many singlets and doublets among the orbits appearing in the right hand sides of eqs.(3.48) and (3.49). E.g., all 0-orbits generated by elements $w : h_L(w) = 0$ and $h_k(w) \geq 1 \ \forall \ k = 1, \ldots, L-1$, are doublets; all 1-orbits generated by configurations $w : h_L(w) = 0$ are singlets. Relations for singlets and doublets provide a number of explicit expressions for stationary state coefficients of the model C. In particular, expressions which are presented in a right column of Table 2 in [17] all correspond to the right 1-singlets. To illustrate the practical use of Conjectures 12 and 8 we shall derive here formulas for stationary state coefficients of configurations

$X(s) :=$ 

(3.52)

where configuration's size L may take even values only and parameter s runs from 1 to $\frac{(L-2)}{2}$. Denote

$Y(s) :=$ 

$Z(s) :=$ 

According to Conjectures 8 and 12 the stationary state coefficients for these configurations and for configurations $W(h_0 = 0, s)$ and $W(h_0 = 1, s)$ (see fig.5 on p.17) satisfy relations

right 0-doublet (eq.(3.48)): $$p_L^{(c)}(Y(s)) + p_L^{(c)}(X(s)) \ = \ \frac{m_L^{(c)} S_{L+2}^{(a)}}{S_L^{(a)}} \, p_L^{(b)}(Y(s)) \, , \quad (s \geq 1) \, ,$$

right 1-singlet (eq.(3.49)): $$p_L^{(c)}(Y(s)) \ = \ m_L^{(c)} \, p_{L+1}^{(b)}(Z(s+1)) \, ,$$

left 0-doublet (first eq.(3.39)): $$p_L^{(b)}(W(0,s)) + p_L^{(b)}(Y(s)) \ = \ S_{L+1}^{(a)} \, S_{L-1,s}^{(a)} \, , \quad (s \geq 1) \, ,$$

left (-1)-singlet (second eq.(3.39)): $$p_L^{(b)}(W(0,s)) \ = \ S_L^{(a)} \, S_{L,s}^{(a)} \, ,$$

left 1-doublet (second eq.(3.40)): $$p_{L+1}^{(b)}(W(1,s+1)) + p_{L+1}^{(b)}(Z(s+1)) \ = \ S_{L+2}^{(a)} \, S_{L,s}^{(a)} \, , \quad (s \geq 1) \, ,$$

left 0-singlet (first eq.(3.40)): $$p_{L+1}^{(b)}(W(1,s+1)) \ = \ S_{L+1}^{(a)} \, S_{L+1,s+1}^{(a)} \, ,$$

wherefrom one obtains

$$p_L^{(c)}(X(s)) \ = \ m_L^{(c)} \left\{ \frac{S_{L+2}^{(a)} \, S_{L+1}^{(a)} \, S_{L-1,s}^{(a)}}{S_L^{(a)}} \ - \ 2 \, S_{L+2}^{(a)} \, S_{L,s}^{(a)} \ + \ S_{L+1}^{(a)} \, S_{L+1,s+1}^{(a)} \right\} . \qquad (3.53)$$

In the last conjecture we describe largest components of the stationary states of the model C.

Conjecture 13 (Model C: maxima). *The maximal coefficient $M_L^{(c)}$ appear in the set $\{p_L^{(c)}\}$ with multiplicity 1 for L even and 2 for L odd.*

For L odd one of the corresponding interface configurations is the substrate shown on Figure 3 c) on page 10. The second one is a mirror image of the first (see Remark 2 to Conjecture 12). For L even the corresponding configuration is $X(1)$ (see def.(3.52)). Explicit values of the maximal coefficients are

$$\textit{for L odd:} \qquad M_L^{(c)} \;=\; m_L^{(c)}\, S_L^{(a)}\, S_{L+2,1}^{(a)}\,, \tag{3.54}$$

$$\textit{for L even:} \qquad M_L^{(c)} \;=\; m_L^{(c)} \left\{ \frac{S_{L+2}^{(a)}\, S_{L-1}^{(a)}\, S_{L+1,1}^{(a)}}{S_L^{(a)}} \;-\; S_L^{(a)}\, S_{L+2,1}^{(a)} \right\}. \tag{3.55}$$

Relation (3.55) is a particular case of eq.(3.53) simplified with the use of Pascal's hexagon relations.

A mirror image of the configuration $X(1)$, which is the substrate, enters the stationary state with next to largest coefficient

$$\textit{for L even:} \qquad p_L^{(c)}(\textit{Substrate}) \;=\; m_L^{(c)}\, S_{L+1}^{(a)}\, S_{L+1,1}^{(a)}\,. \tag{3.56}$$

4 Discussion

Two of the issues discussed in this paper deserve further investigation.

The first one is Pascal's hexagon relation which surprisingly comes as defining recurrent equation for some of the RPM's stationary coefficients. At the moment we do not have explanation to this fact. A very preliminary investigation of Pascal's hexagon relation is carried out in the Appendix. It shows that besides the solution $S_{L,N}^{(a)}$ (3.26) which is related to RPM with open boundaries the relation admits also solutions which manifest themselves in the periodic stochastic models (see eq.(A.8) and the sentence above it; see also remark 4 on page 24). Besides that, an extensive list of relations (A.27)–(A.38)) obtained in the Appendix indicates an existence of a profound relation between solutions of Pascal's hexagon reccurence and combinatorics of the alternating sign matrices. This relation has to be further explored.

Secondly, while studying the stationary states of the models A, B and C we observed close relations between their probability distributions. Similar relations were also observed in Ref.[16] for the spectra of the models. Such relations have been interpreted by introducing the notion of orbits on the space of configurations of the models B and C. These facts suggest an idea that models B and A can be obtained by factorization of the model C.

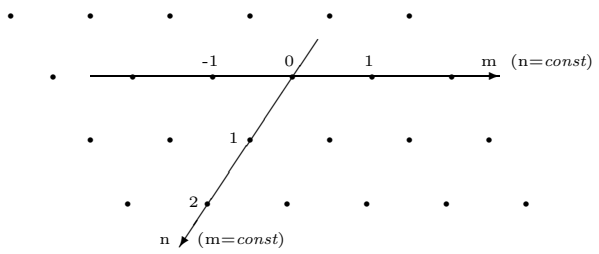
It would be interesting to find out such conjectural factorization at the level of boundary extended Temperley-Lieb algebras.

5 Acknowledgements

The author is grateful to Jan de Gier, Andrey Mudrov, Bernard Nienhuis, Yuri Stroganov and Nikolai Tyurin for useful discussions. Special thanks to Vladimir Rittenberg whose constant interest in the subject and valuable advices provide a lot of inspiration to this work. The work is supported in part by RFBR grant # 03-01-00781 and by the grant of Heisenberg-Landau Foundation. The author gratefully acknowledges warm hospitality of Physikalisches Institut of the University of Bonn and of Lorentz Center at the University of Leiden where this work was completed.

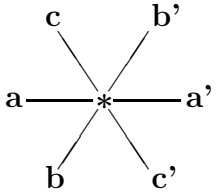
Appendix. Solutions of Pascal's hexagon relation and ASM numbers

Consider a set of numbers which are placed on vertices of a planar trigonal lattice. Introducing coordinate lines on the lattice as it is shown on figure (A.1) we label the numbers in the set by a pair of integers: $\{f_{m,n}\}$, $m, n \in \mathbb{Z}$.



(A.1)

For any six numbers a, a', b, b', c, c' in the set which are situated on apices of a hexagon



(A.2)

we impose a condition

$$aa' + bb' = cc' \,, \tag{A.3}$$

which can be viewed as a generalization of Pascal's triangle relation to the case of hexagon. In coordinatization (A.1) it reads

$$f_{m-1,n}\, f_{m+1,n} \;+\; f_{m,n-1}\, f_{m,n+1} \;=\; f_{m-1,n-1}\, f_{m+1,n+1} \,. \tag{A.4}$$

As the author has learned from Yuri Stroganov Pascal's hexagon relations belong to a wide family of bilinear equations, including Somos sequences, number walls, S-arrays, cube reccurence etc., which are currently extensively investigated in algebraic combinatorics (see, e.g., [27] and references therein; see also bilinear forum on the web). Moreover, it has been mentioned in physical literature under the name of discrete Boussinesq equation (see eq.(8.11) in [26] and the references therein). In [26] it was obtained as certain 2-dimensional reduction of the Hirota's difference equation, which is also called the octahedron reccurence by combinatorialists.

A particular solution of Pascal's hexagon relation is given by formulas

$$f_{m,n} \;=\; 2^{-[n^2/4]} \prod_{p=1}^{n} \frac{1}{(2p-1)!!} \prod_{p=0}^{[\frac{n-1}{3}]} \frac{(m-[\frac{n+p}{2}]-p-1)!}{(m-2n+3p)!} \prod_{p=0}^{[\frac{n-2}{3}]} \frac{(2m+2n-6p-3)!!}{(2m-2[\frac{n+p}{2}]+4p+1)!!}\,, \quad \text{(A.5)}$$

$$f_{-m,-n} \;=\; 2^{-[n^2/4]} \prod_{p=1}^{n-1} \frac{1}{(2p-1)!!} \prod_{p=0}^{[\frac{n}{3}]-1} \frac{(m-[\frac{n+p}{2}]-p-2)!}{(m-2n+3p+2)!} \prod_{p=0}^{[\frac{n-2}{3}]} \frac{(2m+2n-6p-5)!!}{(2m-2[\frac{n+p}{2}]+4p-1)!!}\,, \quad \text{(A.6)}$$

where m is an integer and n is a nonnegative integer. Here for negative values of m ratios of factorials are treated as Pochhammer symbols:

$$(n-1)!/(k-1)! = \prod_{j=k}^{n-1} j \;=:\; (k)_{(n-k)}\,, \qquad (2n-1)!!/(2k-1)!! = 2^{(n-k)}(k)_{(n-k)}(2k)_{(2n-2k)}\,.$$

The corresponding distribution of numbers on the lattice is shown in table 1 on page 32.

Formulas (A.5) and (A.6) can be reproduced in a following way. First, one assigns certain initial data to $f_{m,n}$ (like in Pascal's triangle case)

$$f_{m\geq o,n=0} = 1\,, \qquad f_{m\geq 0,n=-1} = 1\,, \qquad f_{m=2n-1,n>0} = 0\,, \quad \text{(A.7)}$$

and calculates values of $f_{m,n}$ for $n > 0$ and $m \geq 2n$ row by row (i.e., consecutively for $n = 1, 2, 3$, etc.) using relations (A.4). In this way formula (A.5) for detailed distributions $S^{(a)}_{L,n} = f_{m=L,n}$ was obtained in Sec. 3.3.

Then, one observes that formula (A.5) is well defined on a half-plane $n \geq 0$ and gives numbers satisfying Pascal's hexagon relation in this sector. Note that combinatorial functions $R(n, L)$ and $Q(n, L)$ introduced in [17] (see eqs.(16) and (17) there) both are related to function (A.5)

$$f_{m,n} = R(n+1, m+1)\,, \qquad f_{-m,n} = (-1)^{[\frac{n+1}{2}]} Q(n+1, m+n+1)\,. \quad \text{(A.8)}$$

Note also that in the sector $m \leq 2n-1,\ \ n \leq 2m-1$ numbers $f_{m,n}$ vanish (see tab.(1)) that, in particular, destroys the connection between numbers $f_{m,n}$ in sectors $m \geq 2n,\ \ n \geq 0$ and $2m \leq n,\ \ n \geq 0$ via Pascal's hexagon relations.

Further on, comparing numbers $f_{m,n}$ in sectors $m \geq 2n \geq 0$ and $n \geq 2m \geq 0$ one observes $m \leftrightarrow n$ symmetry

$$f_{m,n} = (-1)^{(mn\,+\,[4(m+n)/3])}\, 2^{-[(m-2n)/3]}\, f_{n,m} \quad \forall\, m \geq n \geq 0\,. \tag{A.9}$$

Extrapolating this symmetry relation one defines numbers $f_{m,n}$ in sector $m \geq 0 \geq n$ through those from sector $n \geq 0 \geq m$. The Pascal's hexagon relation for the newly defined numbers stays valid.

Finally, one can guess general formula (A.6) for $f_{m,n}$ on a half-plane $n < 0$ analyzing the numbers in sector $m \geq 0 \geq n$. The numbers $f_{m,n}$ thus obtained satisfy relation (A.4) on the whole lattice. Let us end up discussion of the solution (A.5), (A.6) with a list of remarks.

1. $f_{m,n}$ take particularly simple values along the following directions (see tab.1)

$$f_{m,0} \,=\, f_{m,-1} \,=\, 1 \tag{A.10}$$

$$f_{0,n} \,=\, (-1)^{[4n/3]}\, 2^{[n/3]}\,, \quad f_{0,-n} \,=\, (-1/2)^{[2n/3]}\,, \quad \forall\, n \geq 0\,, \tag{A.11}$$

$$f_{-1,n} \,=\, (-2)^{[(n+2)/3]}\,, \quad f_{-1,-n} \,=\, (-1)^{[(2-n)/3]}\, (1/2)^{[(2n-1)/3]}\,, \quad \forall\, n \geq 1\,, \tag{A.12}$$

$$f_{m=2n-1,n>0} \,=\, f_{m>0,n=2m-1} \,=\, f_{m=2n+3.n<-2} \,=\, f_{m<-2,n=2m+3} \,=\, 0\,. \tag{A.13}$$

   Conditions (A.10)–(A.13) can be used as initial data for reconstruction of all the nonzero numbers $f_{m.n}$ by means of relation (A.4).

2. Symmetry relations (A.9) are valid for any pair m, n such that $m \geq n$ (but not for $m < n$).

3. The numbers $f_{m,n}$ given by eq.(A.5) are always integer. The numbers $f_{-m,-n}$ given by eq.(A.6) become integer upon multiplication by $2^{(n-1)}$. This fact is a particular manifestation of the Laurent property, which was proved in general in [27] (for specialization to the case of octahedron recurrence see [28]). [10]

4. The numbers $f_{m,n}$ in sectors $m \geq 2n \geq 0$ and $0 \leq n \leq 1 - m$ are known to be related to open and periodic one dimensional stochastic models, respectively (see [17] and Sec.3.3). One may expect that there exists some one dimensional stochastic process related to the numbers $f_{m,n}$ in sector $n \leq -1$, $m \leq 2n + 2$.

Next, we consider solutions of Pascal's hexagon relation which are polynomials in one, or several variables. Evaluated at particular values of their variable(s) they produce numeric solutions to (A.4). We found two examples of polynomial solutions.

First one is a set of polynomials in two variables $F_{m,n}(x, y)$ which are defined in the sector $n \geq 0$, $m \geq 2n - 1$. They satisfy Pascal's hexagon relation (A.4) (just substitute

[10] The author is grateful to David Speyer for pointing out this fact to his attention.

$f_{m,n}$ by $F_{m,n}(x,y)$ there) and one can uniquely define them provided that polynomials on the boundaries of the sector are fixed. We choose

$$F_{m>0,0} = 1\,, \qquad F_{m>1,1} = y + (m-2)x\,, \qquad F_{m=2n-1,n>0} = 0\,, \tag{A.14}$$

which is a generalization of boundary conditions (A.7). A nontrivial fact is that with such choice of the boundary conditions one obtains polynomial (rather then rational) expressions for $F_{m,n}(x,y)$. In table 2 on page 33 some polynomials $F_{m,n}(x,y)$ for small values of m and n are listed.

The functions $F_{m,n}(x,y)$ obey rescaling symmetries[11]

$$F_{m,n}(x,y) \;=\; y^n\, F_{m,n}(x/y,1)\,, \qquad \text{for } y \neq 0\,, \tag{A.15}$$

$$F_{m,n}(x,0) \;=\; x^n\, F_{m,n}(1,0)\,, \tag{A.16}$$

$$F_{2n,n}(x,y) \;=\; yF_{2n,n-1}(x,y)\,. \tag{A.17}$$

It follows then that only two values $y = 0$ and $y = 1$ are essential. We keep using variable y as it is suitable for producing integral solutions to Pascal's hexagon relations. In particular, one finds following relations between polynomials $F_{m,n}$ and the numbers given by formulas (A.5) and (A.6)

$$F_{m+1,n}(1,0) \;=\; F_{m+2,n+1}(0,1) \;=\; F_{m,n}(1,1) \;=\; f_{m,n}\,, \tag{A.18}$$

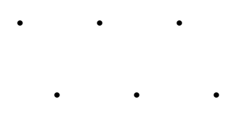
$$F_{m,n}(2,3) \;=\; 2^n f_{-m,-n-1}\,. \tag{A.19}$$

Another set of polynomials $G_{m,n}(x)$ are solutions of a variant of Pascal's hexagon relations

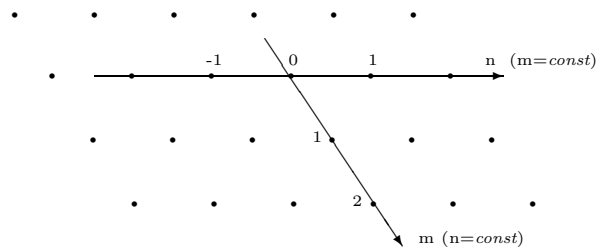
$$G_{m,n+1}G_{m,n-1} + G_{m+1,n-1}G_{m-1,n+1} \;=\; G_{m-1,n}G_{m+1,n}\,. \tag{A.20}$$

These relations result from a different coordinatization of Pascal's hexagon rules (A.2), (A.3).

[11] Rescaling properties (A.15), (A.16) are particular manifestations of "gauge" transformations on the set of solutions of Pascal's hexagon equation. Namely, once a solution $\{a, a', b, b', c, c'\}$ of eq.(A.3) is given a family of gauge equivalent solutions $\{\alpha a, \alpha' a', \beta b, \beta' b', \gamma c, \gamma' c'\}$ is parametrized by six scaling numbers α, α', β, β', γ and γ' satisfying constraints $\alpha\alpha' = \beta\beta' = \gamma\gamma' \neq 0$. On a trigonal lattice this gauge transformation is uniquely defined provided one fixes 6 mutually independent scaling parameters for the vertices situated as shown on a figure



The coordinate frame for them looks as



(A.21)

For this set of functions we impose boundary conditions

$$G_{0,n>0} = 1\,, \quad G_{1,n\geq 0} = 1+nx\,, \quad G_{m>0,0} = x^{[(m+1)/3]}(x+1)^{[m/3]}(-1)^{[m/3]+[m/2]}\,, \quad \text{(A.22)}$$

which allow one to iteratively reconstruct polynomials $G_{m,n}(x)$ (again, a nontrivial fact) in the sector $m \geq 0$, $n \geq 0$. In particular, one finds

$$G_{m,1} = x^{[m/3]}\,(x+1)^{[(m+2)/3]}\,(-1)^{[(m+2)/3]+[(m+1)/2]}\,. \quad \text{(A.23)}$$

Boundary conditions (A.22), (A.23) are generalizations of the boundary data for $f_{m,n}$ along directions $m < 0,\ n \in \{0,1\}$, and $n > 0,\ m \in \{0,-1\}$ (see table 1 and formulae (A.10)–(A.12)). Explicit expressions for $G_{m,n}(a)$ for small values of m and n are given in table 2 on page 33.

The functions $G_{m,n}(x)$ obey reflection symmetry

$$G_{m,n}(x) = x^{[(m-n+1)/3]}\,\tilde{x}^{-[(\tilde{m}-\tilde{n}+1)/3]]}\,(-1)^{[(m+n)/2]}\,G_{\tilde{m},\tilde{n}}(\tilde{x})\,, \quad \text{for } x \neq 0,-1, \quad \text{(A.24)}$$

$$G_{m,n}(0) = (-1)^{m+1}\,G_{m-1,n+1}(-1)\,, \quad \text{(A.25)}$$

where $\tilde{x} = -1-x$, $\tilde{m} = n-1$ and $\tilde{n} = m+1$. At certain values of x they reproduce numbers (A.5)

$$G_{m,n}(0) = f_{m+n-1,m-1}\,, \quad G_{m,n}(1) = (-1)^{[(m+1)/2]}\,f_{-n,m}\,. \quad \text{(A.26)}$$

Finally, it is remarkable that the solutions of Pascal's hexagon relation reproduce in several ways numbers which were discovered in counting various symmetry classes of the alternating sign matrices (see [23, 24, 25]). Below we present list of such formulae. Relations (A.27), (A.28) and (A.31)–(A.34) were observed in [17] (see eqs.(18)–(23) there). First equalities in (A.27) and (A.29) are particular manifestations of eq.(A.17).

$$F_{2n,n-1}(1,1) = F_{2n,n}(1,1) = G_{n+1,n}(0) = G_{n,n+1}(0)$$
$$= \{1,3,26,646,\ldots\} = A^V_{2n+1}\,, \qquad n>0, \quad \text{(A.27)}$$

$$F_{2n-1,n-1}(1,1) = G_{n,n}(0) = \{1,1,2,11,170,\ldots\} = \frac{A^{VH}_{4n\pm 1}}{A^V_{2n\pm 1}}\,, \qquad n\geq 0, \quad \text{(A.28)}$$

$$F_{2n,n-1}(2,3) = \frac{1}{3}F_{2n,n}(2,3) = \{1,7,143,8398,\ldots\} = \frac{A_{2n-1}}{A^V_{2n-1}}, \quad n>0, \qquad (A.29)$$

$$F_{2n+1,n}(2,3) = \{1,5,66,2431,252586,\ldots\} = \frac{A^{HT}_{4n}}{A_{2n}}\,\frac{A^V_{2n\pm1}}{A^{VH}_{4n\pm1}}, \quad n\geq 0, \qquad (A.30)$$

$$G_{n,n}(1) = \{1,2,10,140,5544,\ldots\} = A^{HT}_{2n}, \quad n\geq 0, \qquad (A.31)$$

$$G_{n,n+1}(1) = \{1,3,25,588,39204,\ldots\} = A^{HT}_{2n+1}, \quad n\geq 0, \qquad (A.32)$$

$$G_{n+1,n}(1) = \{1,2,2\times 7,7\times 42,42\times 429,\ldots\} = A_nA_{n+1}, \quad n\geq 0, \qquad (A.33)$$

$$G_{n,n+2}(1) = \{1,2^2,7^2,42^2,429^2,\ldots\} = (A_{n+1})^2, \quad n\geq 0, \qquad (A.34)$$

$$G_{n,n}(-\frac{1}{2}) = \{1,\frac{1}{2},\frac{1}{2^2},\frac{2^2}{2^3},\frac{6^2}{2^4},\frac{33^2}{2^5},\frac{286^2}{2^6}\ldots\} = \frac{(A^{VH}_{2n+1})^2}{2^n}, \quad n\geq 0, \qquad (A.35)$$

$$G_{n+1,n}(-\frac{1}{2}) = \{1,\frac{1}{2},\frac{2}{2^2},\frac{2\times 6}{2^3},\frac{6\times 33}{2^4},\frac{33\times 286}{2^5}\ldots\} = \frac{A^{VH}_{2n+1}A^{VH}_{2n+3}}{2^n}, \quad n\geq 0, \qquad (A.36)$$

$$G_{n,n+1}(-\frac{1}{2}) = \{1,0,\frac{1}{2^2},0,\frac{3^4}{2^4},0,\frac{26^4}{2^6},\ldots\} = \begin{cases} 0 & \text{for } n\geq 1 \text{ odd},\\ \frac{(A^V_{2n+1})^4}{2^n} & \text{for } n\geq 0 \text{ even}, \end{cases} \qquad (A.37)$$

$$G_{n+2,n}(-\frac{1}{2}) = \{\frac{1}{2},\frac{1^3}{2^2},\frac{1^3\times 3}{2^3},\frac{1\times 3^3}{2^4},\frac{3^3\times 26}{2^5},\frac{3\times 26^3}{2^6},\ldots\}$$

$$= \frac{1}{2^{n+1}}(A^V_{4[(n+2)/4]+1})^{p(n+2)}(A^V_{4[n/4]+3})^{p(n)}, \quad n\geq 0, \qquad (A.38)$$

where $p(n)=1,3,3,1,$ if $(n-4[\frac{n}{4}])=0,1,2,3,$ respectively.

Here A_n is a total number of $n\times n$ alternating sign matrices. Notations A^V_n, A^{VH}_n and A^{HT}_n stand, respectively, for numbers of vertically symmetric, vertically and horizontally symmetric and half turn symmetric $n\times n$ alternating sign matrices. Expressions for A^V_{2n+1} and $A^{VH}_{4n\pm1}/A^V_{2n\pm1}$ are given in (3.9) and (3.12). Formulas for A_n and A^{HT}_n are

$$A_n = \prod_{k=0}^{n-1}\frac{(3k+1)!}{(n+k)!}, \quad A^{HT}_{2n} = (A_n)^2\prod_{k=0}^{n-1}\frac{3k+2}{3k+1}, \quad A^{HT}_{2n+1} = \prod_{k=1}^{n}\frac{4}{3}\left(\frac{(3k)!k!}{(2k)!^2}\right)^2. \qquad (A.39)$$

References

[1] Razumov A.V. and Stroganov Yu. G., Spin chains and combinatorics, 2001 *J. Phys. A: Math. Gen.* **34** 3185–3190 [arXiv:math.CO/0012141]

[2] Batchelor M. T., de Gier J. and Nienhuis B., The quantum symmetric XXZ chain at $\Delta = -1/2$, alternating sign matrices and plane partitions, 2001 *J. Phys. A: Math. Gen.* **34** L265-L270 [arXiv:cond-mat/0101385]

[3] Razumov A.V. and Stroganov Yu. G., Spin chains and combinatorics: twisted boundary conditions, 2001 *J.Phys. A: Math. Gen.* **34** 5335–5340 [arXiv:math.CO/0102247]

[4] Razumov A.V. and Stroganov Yu. G., Combinatorial nature of ground state vector of O(1) loop model, 2004 *Theor. Math. Phys.* **138** 333-337, in Russian: *Teor. Mat. Fiz.* **138** 395-400 [arXiv:math.CO/0104216]

[5] Pearce P. A., Rittenberg V. and de Gier J., Critical $Q = 1$ Potts Model and Temperley-Lieb Stochastic Processes, 2001 arXiv:cond-mat/0108051

[6] Razumov A.V. and Stroganov Yu. G., $O(1)$ loop model with differemt boundary conditions and symmetry classes of alternating–sign matrices, 2001 arXiv:math.CO/0108103

[7] de Gier J., Batchelor M. T., Nienhuis B. and Mitra S., The XXZ spin chain at $\Delta = -1/2$: Bethe roots, symmetric functions and determinants, 2002 *J. Math. Phys.* **43** 4135–4146 [arXiv:math-ph/0110011]

[8] Batchelor M. T., de Gier J. and Nienhuis B., The Rotor Model and Combinatorics, 2002 *Int. J. Mod. Phys. B* **16** 1883-1890 [arXiv:math-ph/0204002]

[9] de Gier J., Nienhuis B., Pearce P. A. and Rittenberg V., Stochastic processes and conformal invariance, 2003 *Phys. Rev. E* **67** 016101-016104 [arXiv:cond-mat/0205467]

[10] Pearce P. A., Rittenberg V., de Gier J. and Nienhuis B., Temperley-Lieb stochastic processes, 2002 *J. Phys. A: Math. Gen.* **35** L661–L668 [arXiv:math-ph/0209017]

[11] de Gier J., Loops, matchings and alternating–sign matrices, to appear in *Discr. Math.* [arXiv:math.CO/0211285]

[12] de Gier J., Nienhuis B., Pearce P. A. and Rittenberg V., The raise and peel model of a fluctuating interface, 2004 *J. Stat. Phys.* **114** 1-35 [arXiv:cond-mat/0301430]

[13] Levine Erel and Rittenberg Vladimir, in preparation

[14] Martin P. and Saleur H., 1994 *Lett. Math. Phys.* **30** 189–206

[15] Martin P.P. and Woodcock D., 2000 *J. Algebra* **225** 957-988

[16] de Gier J., Nichols A., Pyatov P. and Rittenberg V., Magic in the XXZ spin chain, in preparation

[17] Mitra S., Nienhuis B., de Gier J. and Batchelor M. T., Exact expressions for correlations in the ground state of the dense $O(1)$ loop model, 2004 arXiv:cond-mat/0401245

[18] Temperley H. N. V. and Lieb E., 1971 *Proc. Roy. Soc. London Ser. A* **322** 251–280

[19] Pasquier V. and Saleur H., Common structures between finite systems and conformal field theories through quantum groups, 1990 *Nucl. Phys.* **B330** 523–556

[20] de Gier J. and Pyatov P., Bethe Ansatz for the Temperley-Lieb loop model with open boundaries, 2004 *J. Stat. Mech.: Theor. Exp.* **03** P002 [arXiv:hep-th/0312235]

[21] Brak R. and Essam J.W., Asymmetric exclusion model and weighted lattice paths, 2003 arXiv:cond-mat/0311153

[22] Alcaraz F.C., Dasmahapatra S. and Rittenberg V., 1998 *J. Phys. A: Math. Gen.* **31** 845

[23] Robbins D.P., Symmetry classes of alternating sign matrices, 2000 arXiv:math.CO/0008045

[24] Kuperberg G., Symmetry classes of alternating-sign-matrices under one roof, 2002 *Ann. of Math.* **156**, no. 3 835–866 [arXiv:math.CO/0008184]

[25] Bressoud D.M., Proofs and Confirmations. The Story of the Alternating Sigh Matrix Conjecture, 1999 *Cambridge University Press*, Cambridge

[26] Zabrodin A., A survey of Hirota's difference equations, 1997 *Theor. Mat. Fiz.* **113** 1347–1392 [arXiv:solv-int/9704001]

[27] Fomin S. and Zelevinsky A., The Laurent phenomenon, 2001 arXiv:math.CO/0104241

[28] Speyer D.E., Perfect Matchings and the Octahedron Recurrence, 2004 arXiv:math.CO/0402452

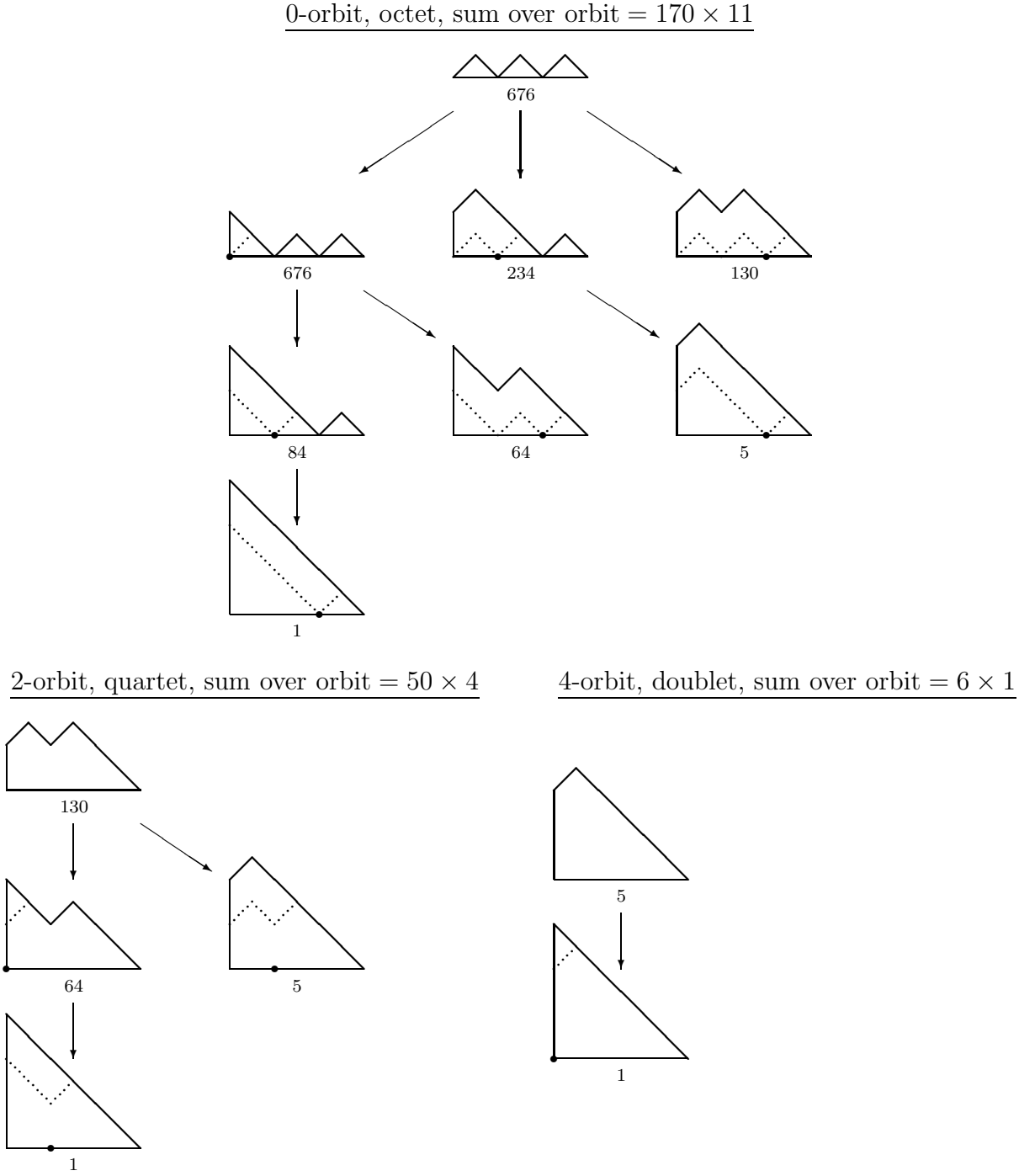


Figure 6: **Examples of maximal left orbits for size $L = 6$ Ballot paths.** Arrows on pictures point from source configurations to their coverings; bold dots indicate points where coverings happen; dashed lines show configuration before covering happen. Numbers standing below configurations are the corresponding stationary state coefficients of the model B. Sums of the coefficients over orbits are described by the first one of relations (3.39).

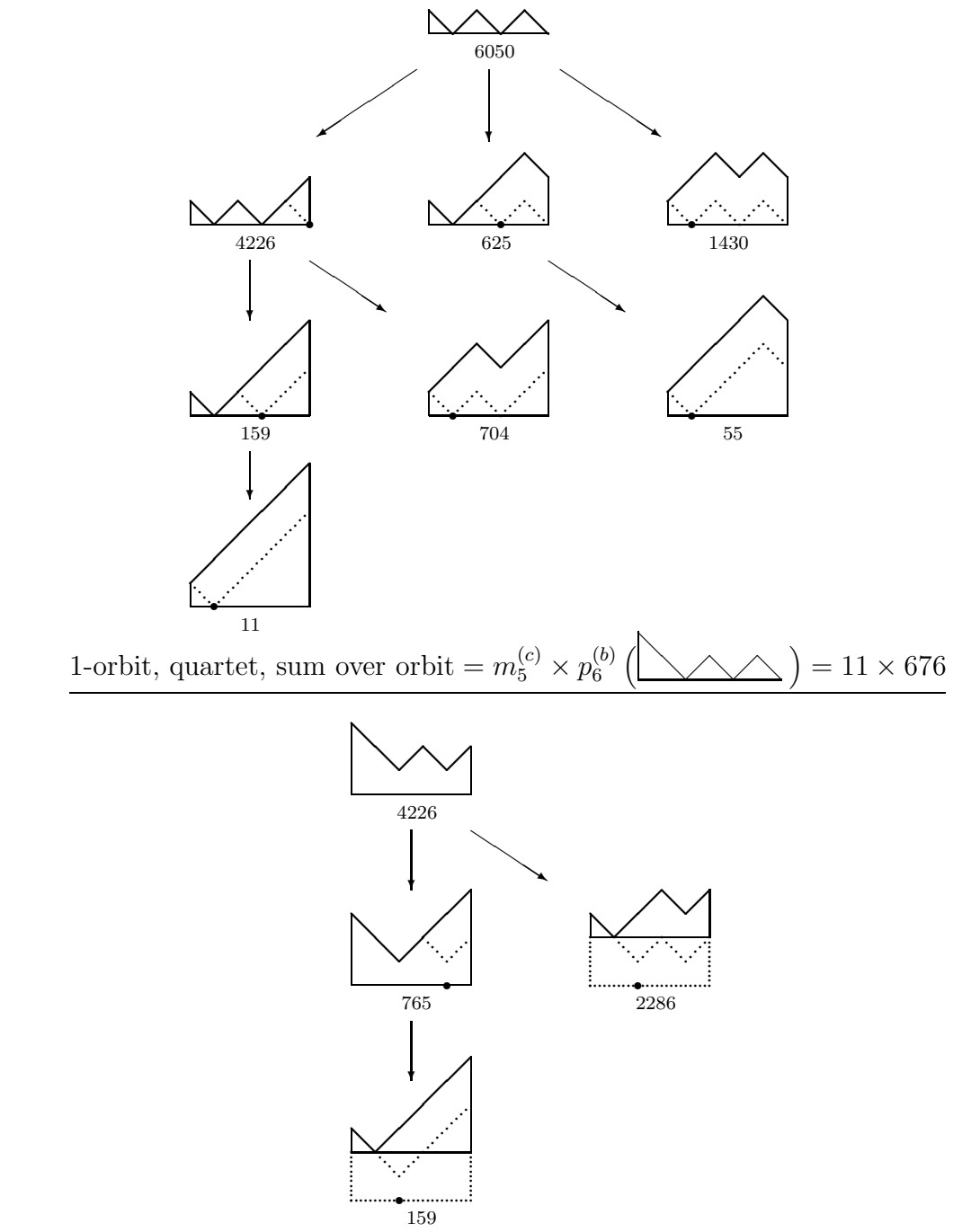


Figure 7: **Examples of maximal right orbits for size $L = 5$ Anchored Cross paths.** Notations are the same as on Fig.6. Numbers standing below configurations are the corresponding stationary state coefficients of the model C. On the last picture two configurations suffer from the total avalanche (3.33).

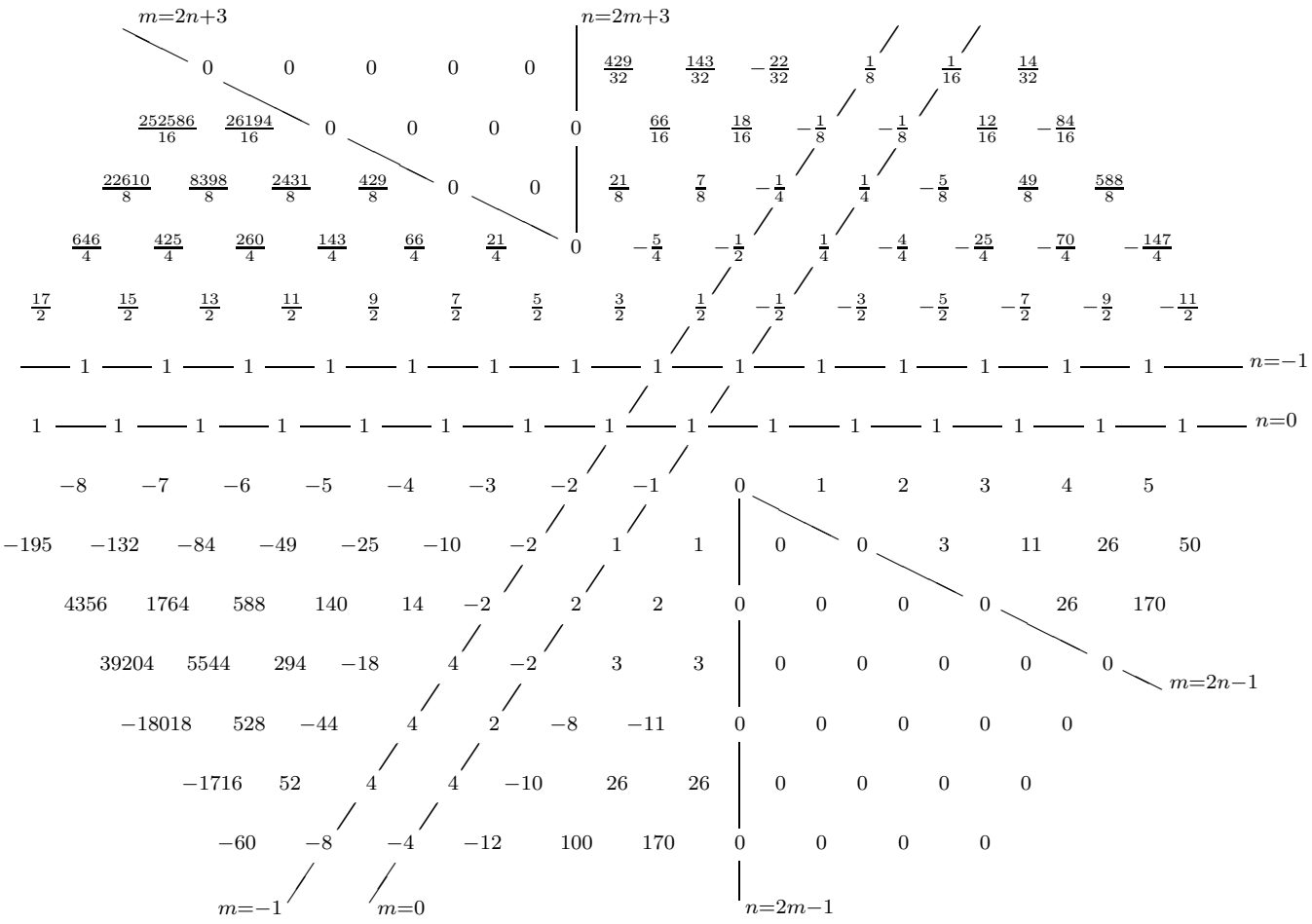


Table 1: Particular solution (A.5), (A.6) of Pascal's hexagon relation (A.4). The numbers standing along indicated lines are given by formulas (A.10)–(A.13). Knowing them one can reconstruct data on the whole lattice by a repeated use of Pascal's hexagon relation.

$$
\begin{aligned}
F_{4,2} &= 2xy + y^2 & \qquad F_{6,3} &= 11x^2y + 12xy^2 + 3y^3 \\
F_{5,2} &= 3x^2 + 6xy + 2y^2 & \qquad F_{7,3} &= 26x^3 + 78x^2y + 55xy^2 + 11y^3 \\
F_{6,2} &= 11x^2 + 12xy + 3y^2 & \qquad F_{8,3} &= 170x^3 + 294x^2y + 156xy^2 + 26y^3 \\
F_{7,2} &= 50x^2 + 30xy + 5y^2 & \qquad F_{9,3} &= 646x^3 + 816x^2y + 350xy^2 + 50y^3 \\
F_{8,2} &= 85x^2 + 42xy + 6y^2 \\
F_{9,2} &= 133x^2 + 56xy + 7y^2
\end{aligned}
$$

$$
\begin{aligned}
F_{8,4} &= 170x^3y + 294x^2y^2 + 156xy^3 + 26y^4 \\
F_{9,4} &= 646x^4 + 2584x^3y + 2839x^2y^2 + 1190xy^3 + 170y^4
\end{aligned}
$$

$$
\begin{aligned}
G_{2,2} &= 2 + 5x + 3x^2 & \qquad G_{3,2} &= 3 + 7x + 4x^2 \\
G_{2,3} &= 3 + 11x + 11x^2 & \qquad G_{3,3} &= 11 + 44x + 59x^2 + 26x^3 \\
G_{2,4} &= 4 + 19x + 26x^2 & \qquad G_{3,4} &= 26 + 137x + 255x^2 + 170x^3 \\
G_{2,5} &= 5 + 29x + 50x^2 & \qquad G_{3,5} &= 50 + 321x + 747x^2 + 646x^3 \\
G_{2,6} &= 6 + 41x + 85x^2
\end{aligned}
$$

$$
\begin{aligned}
G_{4,2} &= -4x - 9x^2 - 5x^3 \\
G_{4,3} &= 26 + 97x + 121x^2 + 50x^3 \\
G_{4,4} &= 170 + 935x + 1956x^2 + 1837x^3 + 646x^4
\end{aligned}
$$

$$
\begin{aligned}
G_{5,2} &= 5x + 16x^2 + 17x^3 + 6x^4 \\
G_{5,3} &= -50x - 179x^2 - 214x^3 - 85x^4
\end{aligned}
$$

$$
G_{6,2} = -6x - 19x^2 - 20x^3 - 7x^4
$$

Table 2: Lattice polynomials $F_{m,n}(x, y)$ and $G_{m,n}(x)$ for small values of m and n.